COMMUNICATIONS IN COMPUTATIONAL PHYSICS
Vol. **3**, No. 1, pp. 121-135

Commun. Comput. Phys.
January 2008

Wave Propagation Simulation Using the CIP Method of Characteristic Equations

Kazuya Shiraishi* and Toshifumi Matsuoka

Department of Civil & Earth Resources Engineering, Kyoto University, Kyotodaigaku-Katsura, Nishikyo-ku, Kyoto 615-8540, Japan.

Received 19 September 2006; Accepted (in revised version) 6 June, 2007

Available online 14 September 2007

Abstract. We apply the CIP (Cubic Interpolated Profile) scheme to the numerical simulation of the acoustic wave propagation based on characteristic equations.The CIP scheme is based on a concept that both the wavefield and its spatial derivative propagate along the same characteristic curves derived from a hyperbolic differential equation. We describe the derivation of the characteristic equations for the acoustic waves from the basic equations by means of the directional splitting and the diagonalization of the coefficient matrix, and establish geophysical boundary conditions. Since the CIP scheme calculates both the wavefield and its spatial derivatives, it is easy to realize the boundary conditions theoretically. We also show some numerical simulation examples and the CIP can simulate acoustic wave propagation with high stability and less numerical dispersion. The method of characteristics with the CIP scheme is a very powerful technique to deal with the wave propagation in complex geophysical problems.

AMS subject classifications: 35L05, 65M25, 81T80

Key words: Acoustic wave, characteristic equation, CIP.

1 Introduction

The Finite Difference method has been widely accepted for wave simulation in solids because of the simplicity of computational implementation. However, careful treatment of the numerical dispersion and computational stability are required in order to obtain the meaningful simulation results. Several advanced techniques are known to reduce numerical dispersion, for example; staggered grids scheme [8] and the high order computation scheme [5]. The pseudo spectra method [3] is also well known as a highly accurate numerical scheme in the Fourier domain. The CIP (Cubic Interpolated Profile)

*Corresponding author. *Email addresses:* skazuya@earth.kumst.kyoto-u.ac.jp (K. Shiraishi), matsuoka@earth.kumst.kyoto-u.ac.jp (T. Matsuoka)

scheme [10, 11] was proposed as a stable and less dispersive scheme in CFD (Computational Fluid Dynamics) and applied to many difficult problems such as the plasma phenomena [4, 11]. The CIP method in combination with the method of characteristics was developed to simulate the Maxwell equation accurately, and it was compared with FDTD method in [6]. The CIP scheme is based on a fact that not only the wavefield but also its spatial derivatives propagate along the same characteristic curve derived from a hyperbolic differential equation.

In this paper we apply the CIP scheme to simulate the P wave propagation by solving an acoustic wave equation. We derive the characteristic equations for the acoustic wave and we solve these equations by the CIP scheme, and establish the treatment of several geophysical boundary conditions such as; the free surface boundary, the irregular topographic boundary, and the absorbing boundary. We also show results of numerical simulations for a simple half space model and topographic variation model.

2 CIP scheme

The phenomenon of the wave propagation in one dimensional space obeys the following first-order differential equation,

$$\frac{\partial f}{\partial t}+u\frac{\partial f}{\partial x}=0. \tag{2.1}$$

This first-order wave equation shows that a wave packet on the wavefield f propagates along a curve $dx/dt=u$ in the phase space. This curve is known as a characteristic curve and Eq. (2.1) is called a characteristic equation for the forward propagation of the wavefield. Although this equation is simple, it is difficult to evaluate numerically with high stability and less numerical dispersion. The CIP scheme can overcome these problems by solving not only (2.1) but also a differential equation for a spatial derivative of the wavefield f. If the propagation velocity u is constant, we obtain the same equation as (2.1) for g which is a spatial derivative of f [10],

$$\frac{\partial g}{\partial t}+u\frac{\partial g}{\partial x}=0, \quad g=\frac{\partial f}{\partial x}. \tag{2.2}$$

These two equations, (2.1) and (2.2), become the governing equations for the propagation of the wavefield f and its spatial derivatives g obey the same characteristic equations. The CIP scheme utilize this property in solving a hyperbolic differential equation and Fig. 1 shows conceptual diagrams of the CIP scheme. In Fig. 1(a), the solid line corresponds to an initial wave packet and dashed line becomes an exact solution at one time-step ahead. Solving the wave equation numerically using the finite difference approximation, we may obtain the white circle (see in Fig. 1(a)) after one time progressed. If the values of the wavefield between the grid points are interpolated linearly using values at each grid, the numerical diffusion occurs shown in Fig. 1(b). However, if we can use the information of the spatial derivatives at every grid points, we can overcome this numerical dispersion problem and may keep the original shape of the wave packet through

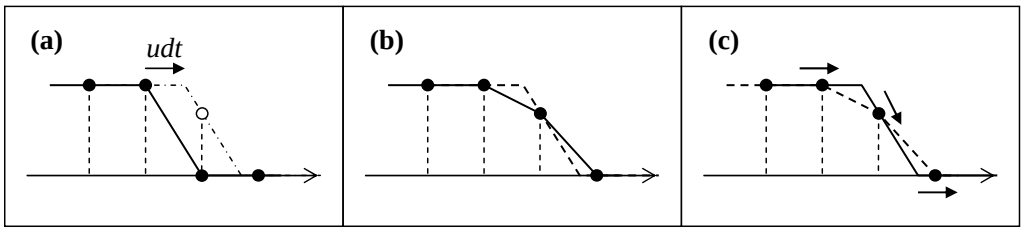

Figure 1: Conceptual diagrams of the CIP scheme (modified from [11]). (a) The solid line corresponds to an initial wave packet and dashed line becomes an exact solution at one time-step ahead. Solving the wave equation numerically using the finite difference approximation, we may obtain the white circle after one time progressed. (b) If the values between the grid points are interpolated linearly using values at each grid, the numerical diffusion occurs (solid line). (c) By using the information of the spatial derivatives (arrows) at every grid points, we can overcome this numerical dispersion problem and may keep the original shape of the wave packet (solid line).

the whole simulation steps. This is the core idea of the CIP scheme and the values at grid points are interpolated using a cubic polynomial (Fig. 1(c)).

If values of the wavefield f and its derivative g are known at two grid points, x_i and x_{i+1}, the wavefield between these two points can be interpolated using a cubic polynomial,

$$F_i^n(x) = a_i\left(x_{iup} - x_i\right)^3 + b_i\left(x_{iup} - x_i\right)^2 + g_i^n\left(x_{iup} - x_i\right) + f_i^n, \tag{2.3}$$

$$a_i = \frac{g_i^n + g_{iup}^n}{D^2} + \frac{2\left(f_i^n - f_{iup}^n\right)}{D^3}, \tag{2.4}$$

$$b_i = \frac{3\left(f_{iup}^n - f_i^n\right)}{D^2} - \frac{2g_i^n + g_{iup}^n}{D}. \tag{2.5}$$

Here, $D = -\Delta x$, $iup = i - 1$ for $u \geq 0$ (forward propagation) and $D = \Delta x$, $iup = i + 1$ for $u < 0$ (backward propagation). From above equations, the profiles of f and g at the $n+1$ step are obtained by shifting the previous profiles by $u_i\Delta t$; $f_i^{n+1} = F_i^n(x_i - u_i\Delta t)$ and $g_i^n = dF_i^n(x_i - u_i\Delta t)/dx$,

$$f_i^{n+1} = a_i\xi_i^3 + b_i\xi_i^2 + g_i^n\xi_i + f_i^n, \tag{2.6}$$

$$g_i^{n+1} = 3a_i\xi_i^2 + 2b_i\xi_i + g_i^n, \tag{2.7}$$

$$\xi_i = -u_i\Delta t. \tag{2.8}$$

We can summarize the CIP scheme as follows; the wavefield is interpolated by a cubic polynomial and it is shifted to the wave propagation direction by $u_i\Delta t$ at each time step.

In order to investigate stability and dispersion features of the CIP scheme, we compare with other numerical schemes such as the first order up-wind scheme (UPW), Lax-Wendroff scheme (LXW), the second order central difference scheme (FDC), and Crank-Nicholson scheme (C-N). Fig. 2 shows simulation results for the one-way wave propagation of a square wave packet which has sharp discontinuous edges and flat part. We set

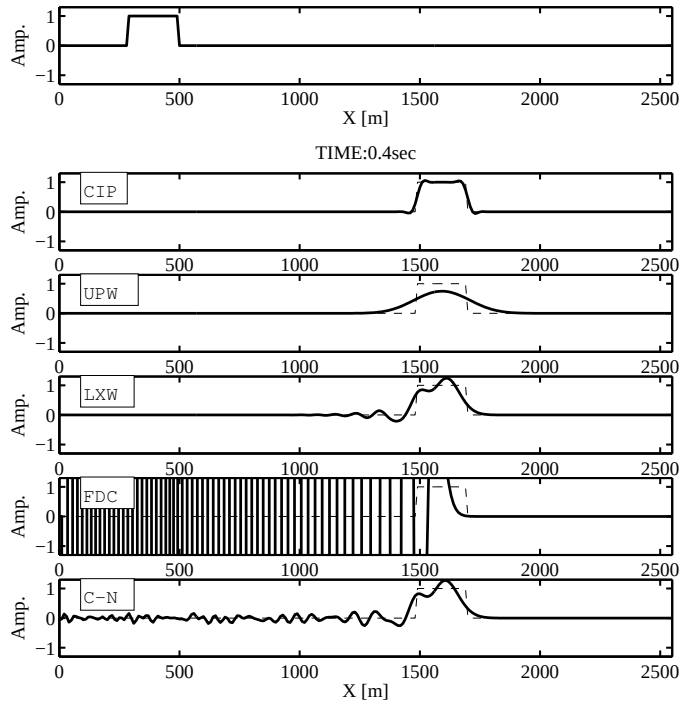

Figure 2: Numerical simulation of one-way wave equation for a square wave (top) with five difference schemes; the CIP scheme (CIP), the first-order up-wind schema, Lax-Wendroff scheme (LXW), central difference scheme (FDC), and Crank-Nicolson scheme (C-N). Solid lines show the simulation results and dashed lines show the exact solution.

$\Delta x = 10$m with 256 grids, $\Delta t = 0.001$s, and $u = 3{,}000$m/s ($u\Delta t/\Delta x = 0.30$). As an initial condition, we set $f(x) = 1$ ($300\text{m} \leq x \leq 500\text{m}$) and $f(x) = 0$ ($x < 300$m and $x > 500$m). In the figure, solid lines show the simulation results and dashed lines show the exact solution. The CIP scheme mostly keeps the shape of the initial waveform. however the UPW scheme shows the numerical diffusion and the LXW scheme and the C-N scheme show the numerical dispersions. The FDC is not stable for this problem. This figure shows that the CIP scheme has the best results with stable and little numerical dispersion even in the case where the input wavelet has high frequency.

3 Characteristic equation for acoustic wave propagation

In applying the CIP scheme to three-dimensional acoustic wave propagation, we rewrite governing equations for the wave motion into combined one-way wave equations. These equations correspond to the characteristic equations describing the acoustic wave propagation in three-dimensional space. As is well known, the equation of continuity and the equation of motion in an acoustic medium are expressed using pressure P and particle

velocity **v** as

$$\frac{\partial P}{\partial t}+\kappa\nabla\cdot\mathbf{v}=0, \tag{3.1}$$

$$\frac{\partial \mathbf{v}}{\partial t}+\frac{1}{\rho}\nabla P=0. \tag{3.2}$$

In these equations, κ is bulk modulus, ρ is density, and $\nabla=(\partial/\partial x,\partial/\partial y,\partial/\partial z)$. We can rewrite these equations in a matrix form with matrices **A**, **B**, and **C**, which are 4×4 matrices including the bulk modulus and the density,

$$\frac{\partial}{\partial t}\begin{bmatrix} P \\ \mathbf{v} \end{bmatrix}+\mathbf{A}\frac{\partial}{\partial x}\begin{bmatrix} P \\ \mathbf{v} \end{bmatrix}+\mathbf{B}\frac{\partial}{\partial y}\begin{bmatrix} P \\ \mathbf{v} \end{bmatrix}+\mathbf{C}\frac{\partial}{\partial z}\begin{bmatrix} P \\ \mathbf{v} \end{bmatrix}=\mathbf{0}, \tag{3.3}$$

where

$$\begin{bmatrix} P & \mathbf{v} \end{bmatrix}^{-1}=\begin{bmatrix} P & v_x & v_y & v_z \end{bmatrix}^{-1},$$

$$\mathbf{A}=\begin{bmatrix} 0 & \kappa & 0 & 0 \\ 1/\rho & 0 & 0 & 0 \\ 0 & 0 & 0 & 0 \\ 0 & 0 & 0 & 0 \end{bmatrix},\quad \mathbf{B}=\begin{bmatrix} 0 & 0 & \kappa & 0 \\ 0 & 0 & 0 & 0 \\ 1/\rho & 0 & 0 & 0 \\ 0 & 0 & 0 & 0 \end{bmatrix},\quad \mathbf{C}=\begin{bmatrix} 0 & 0 & 0 & \kappa \\ 0 & 0 & 0 & 0 \\ 0 & 0 & 0 & 0 \\ 1/\rho & 0 & 0 & 0 \end{bmatrix}.$$

Since the CIP scheme requires the interpolation of the wave field and its shifting of the wavefields and the spatial derivatives, we adopt direction splitting [7,9] and rewrite this equation into three separate independent equations with the diagonalized matrices in (x,y,z) directions. At first, we separate Eq. (3.3) in three directions as follows,

$$\frac{\partial}{\partial t}\begin{bmatrix} P \\ \mathbf{v} \end{bmatrix}+\mathbf{A}\frac{\partial}{\partial x}\begin{bmatrix} P \\ \mathbf{v} \end{bmatrix}=\mathbf{0}, \tag{3.4}$$

$$\frac{\partial}{\partial t}\begin{bmatrix} P \\ \mathbf{v} \end{bmatrix}+\mathbf{B}\frac{\partial}{\partial y}\begin{bmatrix} P \\ \mathbf{v} \end{bmatrix}=\mathbf{0}, \tag{3.5}$$

$$\frac{\partial}{\partial t}\begin{bmatrix} P \\ \mathbf{v} \end{bmatrix}+\mathbf{C}\frac{\partial}{\partial z}\begin{bmatrix} P \\ \mathbf{v} \end{bmatrix}=\mathbf{0}. \tag{3.6}$$

Then, we diagonalize the matrices **A**, **B**, and **C**. Here we show the derivation of the characteristic equations in x direction from Eq. (3.4). Solving the eigenvalue problem, we can rewrite the matrix **A** using a diagonal matrix **M**,

$$\mathbf{A}=\mathbf{L}\mathbf{M}\mathbf{L}^{-1}. \tag{3.7}$$

By substituting this relation into Eq. (3.4), we can finally obtain the following matrix equation containing the pressure and the particle velocities which are propagating in the forward and backward x direction,

$$\frac{\partial}{\partial t}\mathbf{L}^{-1}\begin{bmatrix} P \\ \mathbf{v} \end{bmatrix}+\mathbf{M}\frac{\partial}{\partial x}\mathbf{L}^{-1}\begin{bmatrix} P \\ \mathbf{v} \end{bmatrix}=\mathbf{0}, \tag{3.8}$$

where

$$\mathbf{M}=\begin{bmatrix} \sqrt{\kappa/\rho} & 0 & 0 & 0 \\ 0 & -\sqrt{\kappa/\rho} & 0 & 0 \\ 0 & 0 & 0 & 0 \\ 0 & 0 & 0 & 0 \end{bmatrix},\ \mathbf{L}^{-1}=\frac{1}{2}\begin{bmatrix} 1/\sqrt{\rho\kappa} & 1 & 0 & 0 \\ -1/\sqrt{\rho\kappa} & 1 & 0 & 0 \\ 0 & 0 & 0 & 0 \\ 0 & 0 & 0 & 0 \end{bmatrix}.$$

Finally in the three-dimensional case, we derive the following characteristic equations for the acoustic wave propagation, in x direction,

$$\frac{\partial}{\partial t}\left[+P+I_p v_x\right]+V_p\frac{\partial}{\partial x}\left[+P+I_p v_x\right]=0, \tag{3.9}$$

$$\frac{\partial}{\partial t}\left[-P+I_p v_x\right]-V_p\frac{\partial}{\partial x}\left[-P+I_p v_x\right]=0, \tag{3.10}$$

in the y direction,

$$\frac{\partial}{\partial t}\left[+P+I_p v_y\right]+V_p\frac{\partial}{\partial y}\left[+P+I_p v_y\right]=0, \tag{3.11}$$

$$\frac{\partial}{\partial t}\left[-P+I_p v_y\right]-V_p\frac{\partial}{\partial y}\left[-P+I_p v_y\right]=0, \tag{3.12}$$

and in the z direction,

$$\frac{\partial}{\partial t}\left[+P+I_p v_z\right]+V_p\frac{\partial}{\partial z}\left[+P+I_p v_z\right]=0, \tag{3.13}$$

$$\frac{\partial}{\partial t}\left[-P+I_p v_z\right]-V_p\frac{\partial}{\partial z}\left[-P+I_p v_z\right]=0. \tag{3.14}$$

Here, $I_p=\sqrt{\rho\kappa}=\rho V_p$ is an acoustic impedance, $V_p=\sqrt{\kappa/\rho}$ is the P-wave velocity. Eqs. (3.9) and (3.10) respectively show the forward propagation of $\{+P+I_p v_x\}$ and the backward propagation of $\{-P+I_p v_x\}$ in the x direction. Eqs. (3.9) to (3.14) represent the characteristic equations of the acoustic wave propagation in three-dimensions.

4 Acoustic wave simulation by the CIP scheme

4.1 The CIP scheme on the characteristic equations

In the modeling of acoustic waves based on the method of characteristics, Eqs. (3.9) to (3.14) have to be evaluated numerically. The details of numerical treatments of Eqs. (3.9) and (3.10) using the CIP scheme are shown here. The forward propagation of $\{+P+I_p v_x\}$ and the backward propagation of $\{-P+I_p v_x\}$ are calculated from Eqs. (3.9) and (3.10) respectively;

$$\left[+P^n+I_p\cdot v_x^n\right] \quad\longrightarrow\quad \left[+P^+ + I_p\cdot v_x^+\right], \tag{4.1}$$

$$\left[-P^n+I_p\cdot v_x^n\right] \quad\longrightarrow\quad \left[-P^- + I_p\cdot v_x^-\right]. \tag{4.2}$$

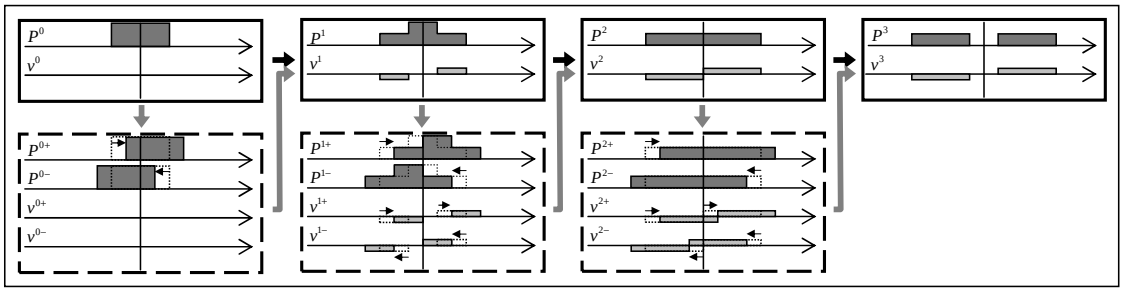

Figure 3: Schematic diagrams of calculation of acoustic wave propagation by method of characteristics. The wavefields at next time step $\{P^{n+1}, v^{n+1}\}$ can be calculated by adding or subtracting the forward and backward wavefields $\{P^{n+},P^{n-},v_x^{n+},v_x^{n-}\}$ according to Eqs. (4.3) and (4.4).

Here superscripts $^+$ and $^-$ mean the forward and the backward propagation. Then we obtain the wavefield at the $n+1$ th step by linear summation of the forward and the backward wavefields;

$$P^{n+1} = \frac{1}{2}\left[\left(P^+ + P^-\right) + \left(v_x^+ - v_x^-\right)\cdot I_p\right], \tag{4.3}$$

$$v_x^{n+1} = \frac{1}{2}\left[\left(v_x^+ + v_x^-\right) + \left(P^+ - P^-\right)/I_p\right]. \tag{4.4}$$

The pressure P and the particle velocity v_x are related by the acoustic impedance I_p. Acoustic wave propagation is described not only by the pressure but also by the particle velocity that are related by the acoustic impedance each other. Fig. 3 show physical meaning of Eqs. (4.3) and (4.4). In calculation of acoustic wave propagating in two directions, we calculate both forward and backward wavefields $\{P^{n+},P^{n-},v_x^{n+},v_x^{n-}\}$, from $\{P^n,v_x^n\}$, and then we obtain the wavefield at next time step $\{P^{n+1},v_x^{n+1}\}$ by adding or subtracting them according to Eqs. (4.3) and (4.4). In addition, their spatial derivatives are also calculated by the same relationship as above equations,

$$\partial_x P^{n+1} = \frac{1}{2}\left[\left(\partial_x P^+ + \partial_x P^-\right) + \left(\partial_x v_x^+ - \partial_x v_x^-\right)\cdot I_p\right], \tag{4.5}$$

$$\partial_x v_x^{n+1} = \frac{1}{2}\left[\left(\partial_x v_x^+ + \partial_x v_x^-\right) + \left(\partial_x P^+ - \partial_x P^-\right)/I_p\right]. \tag{4.6}$$

Here, we defined ∂_x as a spatial derivative $\partial/\partial x$.

The total wavefield in a multi-dimensional medium is calculated by the characteristic equations of each direction in order. In the three-dimensional case, at first we calculate the wavefields propagated in x direction $[P^*,\mathbf{v}^*]$ by solving Eq. (3.4) from $[P^n,\mathbf{v}^n]$, and then we calculate the wavefields propagated in y direction $[P^{**},\mathbf{v}^{**}]$ using the result $[P^*,\mathbf{v}^*]$ by Eq. (3.5), and finally we obtain the wavefield at the next step $[P^{n+1},\mathbf{v}^{n+1}]$ by solving Eq. (3.6) using the wavefields $[P^{**},\mathbf{v}^{**}]$. Fig. 4 shows an snapshot of a numerical simulation in a three-dimensional homogeneous medium ($V_p = 3{,}000\mathrm{m/s}$, $\rho = 2.0\mathrm{g/cm}^3$) when the pressure (Ricker wavelet: $f_{peak} = 100\mathrm{Hz}$) is applied as a source at the center.

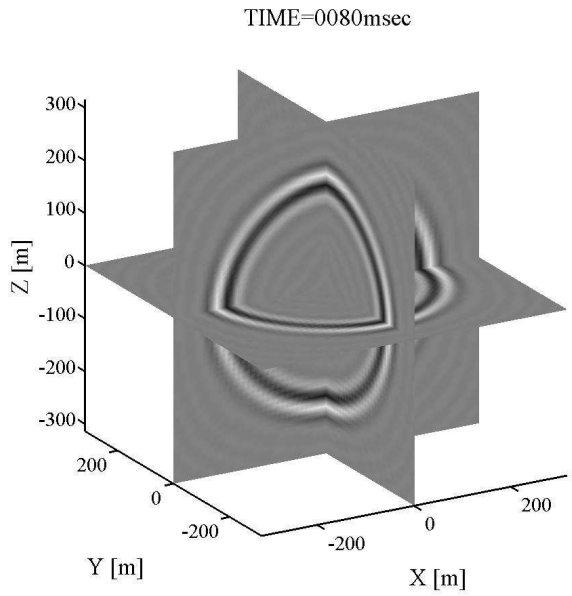

Figure 4: Acoustic wave propagation in a three-dimensional homogeneous medium; snapshot at 0.080s.

Grid spacing is $\Delta x=\Delta y=\Delta z=10$m with $NX\times NY\times NZ=64\times 64\times 64$ grids, and time interval is $\Delta t=0.001$s ($V_p\Delta t/\Delta x=0.3$).

4.2 Boundary condition

For the simulation of wave propagation in geophysical problems, we need to set some boundary conditions such as a free surface boundary (e.g. earth surface) and a transparent/absorbing boundary (e.g. to realize a semi-infinite medium). The boundary conditions are generally described using the physical values $\{P,v_j\}$ and their spatial derivatives $\{\partial P/\partial x_i,\partial v_j/\partial x_k\}$. Therefore, in the simulation scheme based on the characteristic equation with the CIP, it is easy to handle these boundary conditions in comparison with other numerical schemes.

Here we show treatments of three kinds of boundary conditions; a free surface boundary, a symmetric boundary, and a transparent/absorbing boundary, and also we mention handling a topographic variation boundary. To simplify the problems, we treat a two-dimensional case and we assume the boundary is located at $z=j\Delta z$ (see Fig. 5(a)).

Free surface

The free surface is the most important boundary for the geophysical applications. The free surface conditions are expressed as

$$P=0,\quad \frac{\partial v_x}{\partial z}=0,\quad \frac{\partial v_z}{\partial z}=0. \tag{4.7}$$

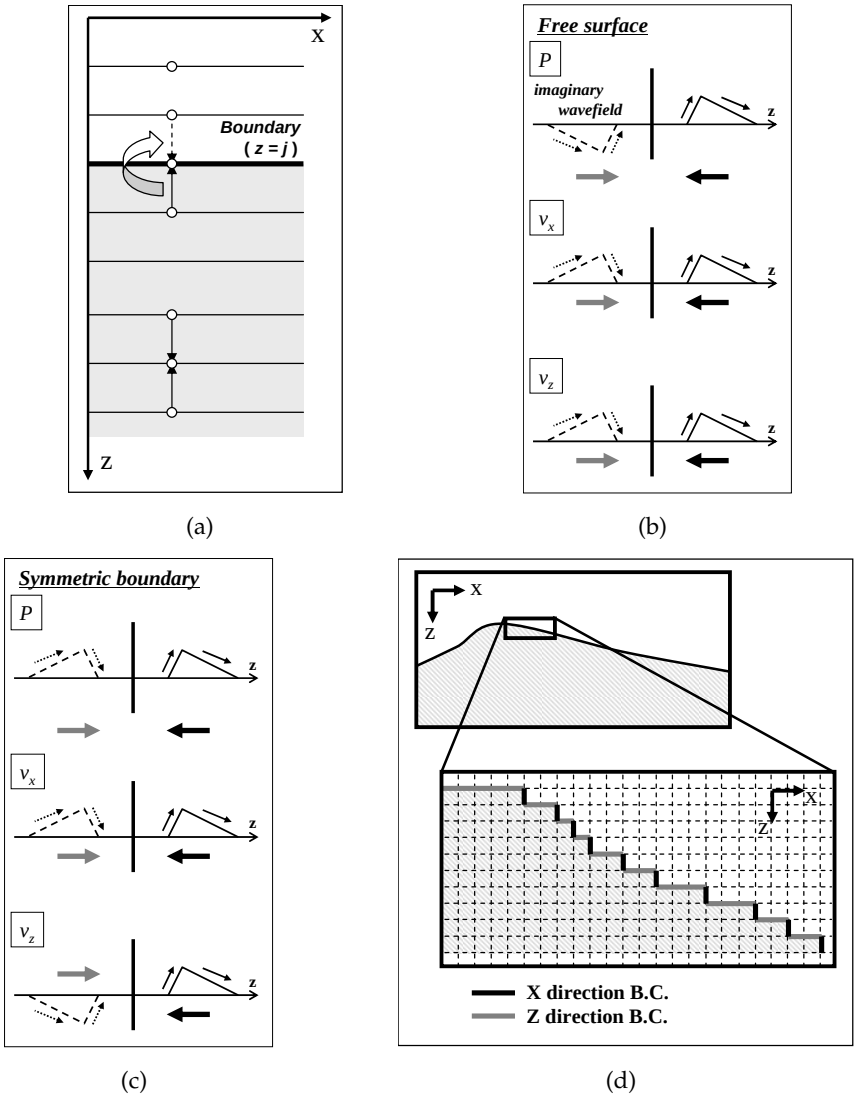

Figure 5: Boundary condition. (a) Down-going wavefield is replaced by up-going wavefield. (b) The sign of the up-going and down-going wavefields at the free surface and (c) the symmetric boundary. (d) Calculation of topographic boundary condition.

In order to realize these conditions, let us introduce the concept of a mirrored imaginary wavefield. When we calculate the pressure and the particle velocity at the free surface using underground wave and mirrored imaginary wave above the surface with opposite or same sign respectively (see Fig. 5(b)), the above free surface boundary conditions are satisfied automatically. We need to pay attention of the sign of both the physical values and the spatial derivatives. From the calculation process at the $n+1$ th wavefield represented in Eqs. (4.3) to (4.6), we need to prepare the wavefield propagating forward and

backward. To satisfy the conditions in Eq. (4.7), we set the forward propagated wavefield by using the backward propagated wavefield as follows; for the pressure,

$$P^+ = -P^-, \quad \partial_z P^+ = \partial_z P^-, \tag{4.8}$$

and for the particle velocity,

$$v_x^+ = v_x^-, \quad v_z^+ = v_z^-, \quad \partial_z v_x^+ = -\partial_z v_x^-, \quad \partial_z v_z^+ = -\partial_z v_z^-. \tag{4.9}$$

Symmetric boundary

The symmetric boundary is occasionally useful to deal with the geophysical problem. For example, when we simulate two- or three-dimensional full wave propagation in one-dimensional stratified media, it is enough to calculate the wave propagation only in half of the media. For a line symmetric boundary (Fig. 5(c)), we can define the conditions,

$$\frac{\partial P}{\partial z} = 0, \quad \frac{\partial v_x}{\partial z} = 0, \quad v_z = 0. \tag{4.10}$$

To satisfy the conditions in Eq. (4.10), we set the forward propagated wavefield by using the backward propagated wavefield as follows; for the pressure,

$$P^+ = P^-, \quad \partial_z P^+ = -\partial_z P^-, \tag{4.11}$$

and for the particle velocity,

$$v_x^+ = v_x^-, \quad v_z^+ = -v_z^-, \quad \partial_z v_x^+ = -\partial_z v_x^-, \quad \partial_z v_z^+ = \partial_z v_z^-. \tag{4.12}$$

Transparent/absorbing boundary

The CIP scheme naturally satisfies transparent/absorbing boundary conditions in an orthogonal direction to the boundary, because it is solving the one-way wave equations for a given simulation models. It is not necessary to consider special treatment at these boundaries of the models. However, oblique incident waves with high angle at edges dose not disappear perfectly. Especially, S wave with high incident angle reflect/refract at the edge. This is a well-known problem in the conventional boundary condition based on the approximation of the one-way wave propagation, too [2]. The easiest way to avoid this difficulty is to combine the absorbing boundary by damping amplitude of waves near the edges [1] with the transparent boundary conditions.

Topographic boundary

If we use rectangular grid mesh in the wave modeling, irregularity of topography is represented as a step boundary (Fig. 5(d)), and they are classified into vertical free surface boundaries and the horizontal free surface boundaries respectively. However, in the CIP scheme the boundary conditions can be treated easily since the wavefields are propagated along two characteristic equations (x and z directions).

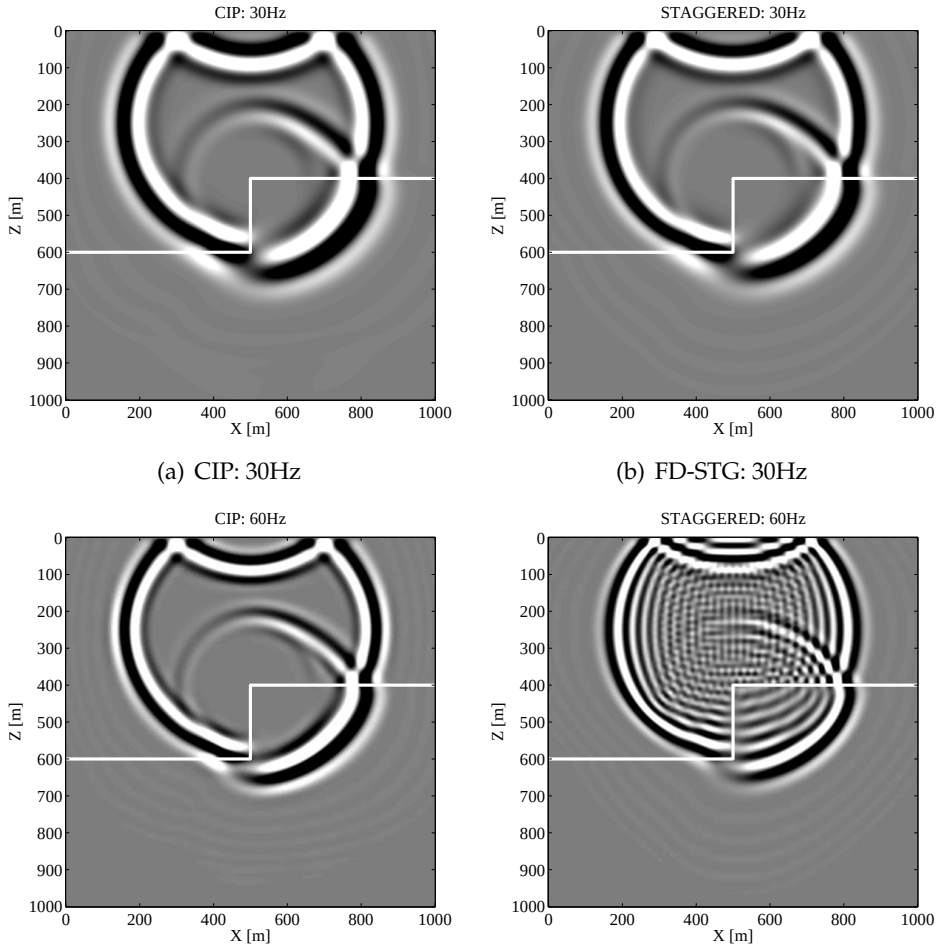

(a) CIP: 30Hz (b) FD-STG: 30Hz

(c) CIP: 60Hz (d) FD-STG: 60Hz

Figure 6: Comparison of the CIP scheme and the FD-STG scheme, and different frequencies of the source wavelet (snapshots at $t = 0.20$s).

5 Numerical examples

5.1 Simple step structure model

We simulate the wave propagation in a step structure model using the characteristic equation with the CIP scheme and compare simulation results with the results of the conventional finite difference scheme with staggered grids (FD-STG) that approximates the equations of motion and continuity by the fourth-order operator. The FD-STG method is widely used in computational geophysics [5, 8]. The 101×101-grid model has a step boundary (white line in Fig. 6) with grid spacing $\Delta x = \Delta z = 10$m, and the model properties are $V_p = 3{,}000$m/s and $\rho = 1.5$g/cm^3 in the upper layer, and $V_p = 4{,}000$m/s and

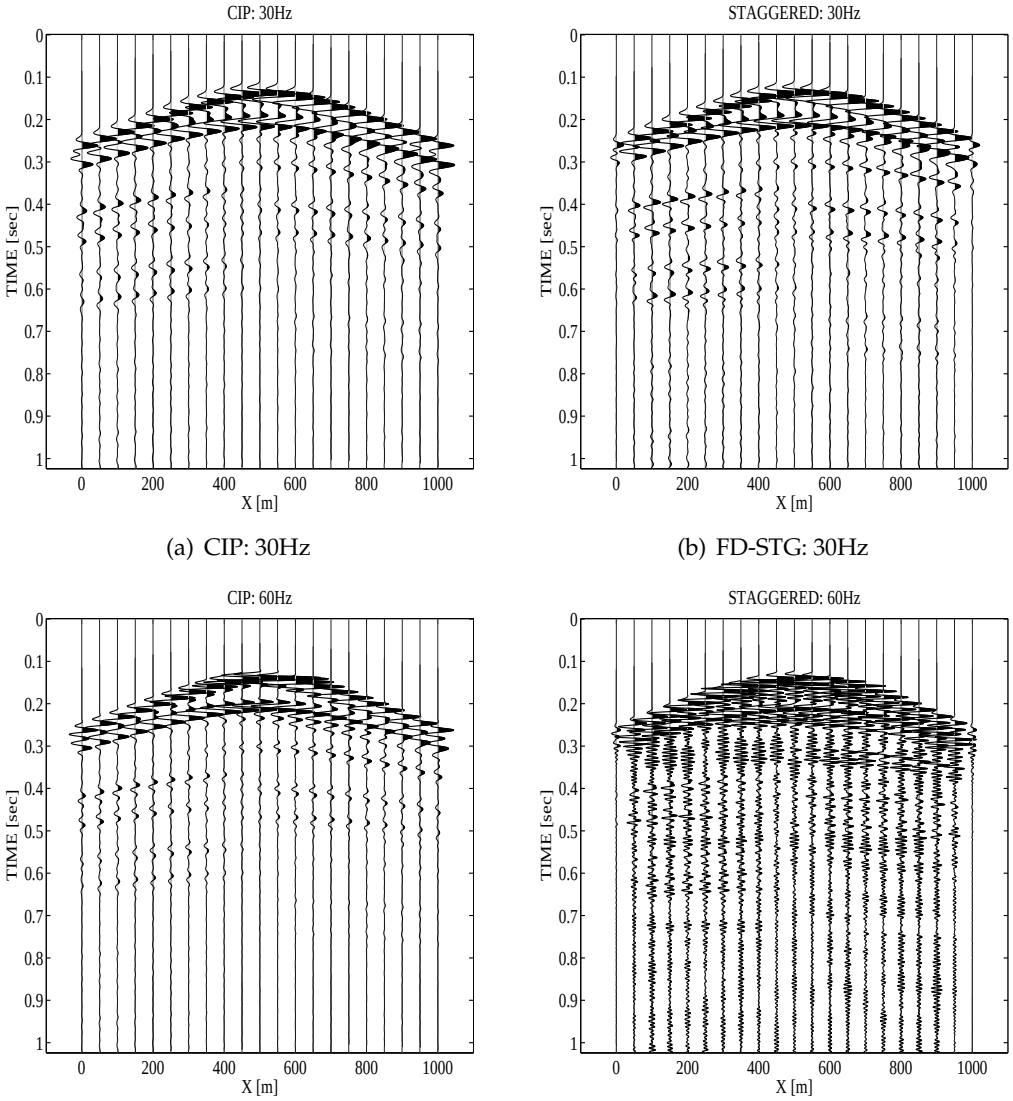

(a) CIP: 30Hz

(b) FD-STG: 30Hz

(c) CIP: 60Hz

(d) FD-STG: 60Hz

Figure 7: Comparison of the CIP scheme and the FD-STG scheme, and different frequencies of the source wavelet (synthetic seismograms)

$\rho = 2.5\text{g/cm}^3$ in the lower layer. An explosive source is located at $(x,z) = (500\text{m},200\text{m})$, and receivers are deployed $(x,z) = (0\text{m},100\text{m}) \sim (10000\text{m},100\text{m})$ with 50m spacing. The source waveform is Ricker wavelet and we simulate two cases with different peak frequencies, 30Hz and 60Hz, to evaluate the numerical dispersion. The time interval in the calculation is $\Delta t = 0.001\text{s}$.

Fig. 6 shows snapshots at $t = 0.20\text{s}$, and Fig. 7 shows synthetic seismograms. Obvi-

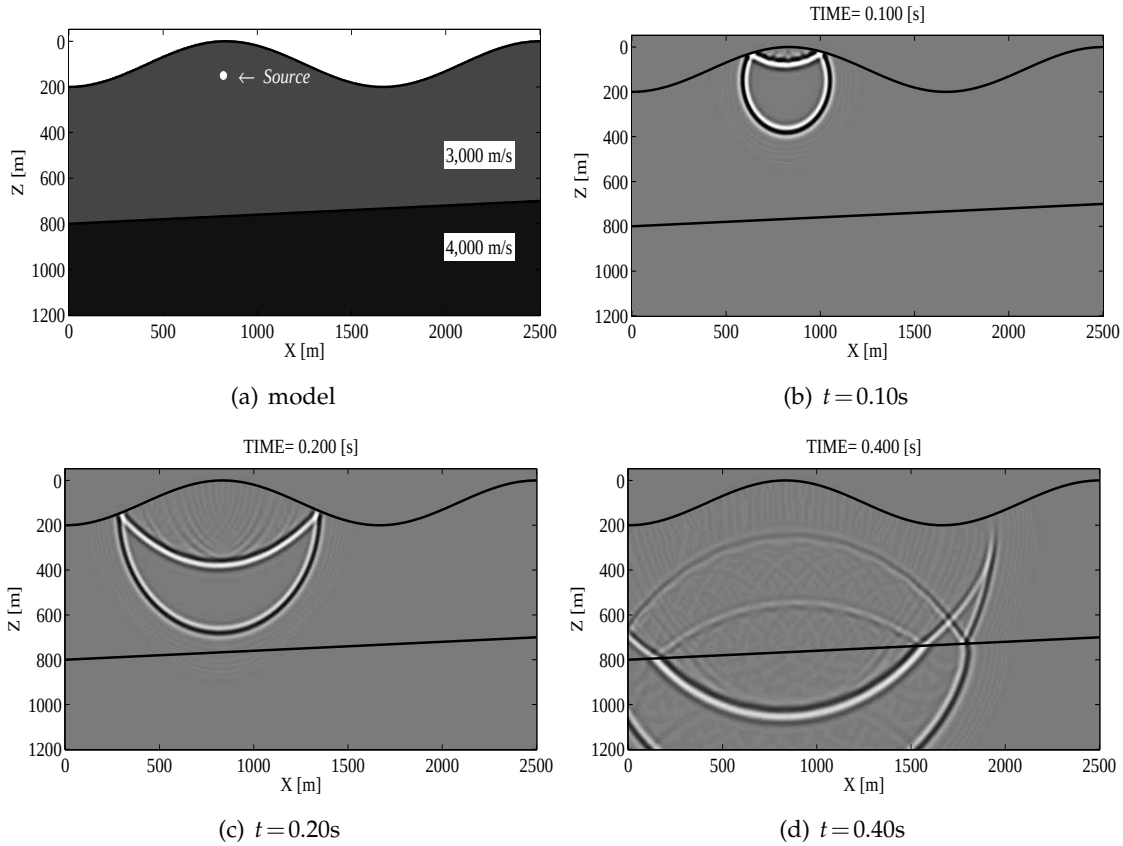

(a) model (b) $t=0.10$s

(c) $t=0.20$s (d) $t=0.40$s

Figure 8: Wave simulation in a topographic medium (a), and snapshot of the wavefield at $t=0.10$s (b), $t=0.20$s (c), and at $t=0.40$s (d) after source generation. Waves are reflected at the topographic free surface with opposite phase, and reflected and transmitted at the subsurface boundary with coordinate phase.

ously, even if the wave length is relatively short compare to the grid distance the CIP scheme can simulate the wave propagation with far less numerical dispersion than the FD-STG. However, our code developed in this study takes more computation cost, time and memory. The calculation time by our CIP scheme required about ten times of that of by FD-STG. This result shows that the CIP scheme with the regular mesh grid can simulate the wave propagation with smaller number of grids than the finite difference scheme with the staggered grid.

5.2 Topographic media

We simulate the wave propagation in the model with the topographic variation. In the model in Fig. 8, the free surface has a sinusoidal wavy variation of the topography, and the boundary between the upper layer and the lower layer is slightly inclined. Model properties are $V_p=3{,}000$m/s, $\rho=2{,}500$ kg/m^3 in the upper layer, and $V_p=4{,}000$m/s, $\rho=$

3,000 kg/m^3 in the lower layer. The compressional source (Ricker wavelet: $f_{peak}=60Hz$) is applied at (x,z)=(820m,150m). Grid spacing is Δx=Δz=5m with $NX \times NZ$=501 $\times$ 251 grids, and time interval is $\Delta t=0.0005$s.

Figs. 8(b)-8(d) shows snapshots of wavefield at different time; $t=0.10$s, $t=0.20$s, and $t=0.40$s. We can recognize the propagation of reflected waves at the surface along the varied topography, and reflected and transmitted waves at the subsurface boundary. In addition, the transparent boundary works well. Our boundary conditions work appropriately even in the geophysical model with the topographic variation.

6 Discussions

We applied the CIP scheme to the numerical simulation of the acoustic wave propagation based on characteristic equations in geophysical problems. The characteristic equations for the acoustic waves are derived from the basic equations of motion and continuity by means of the directional splitting and the diagonalization of the coefficients matrix. For the realistic wavefield modeling, we established several boundary conditions in this method. Since the CIP scheme calculates the propagation of both physical values and their spatial derivatives also, we can simulate acoustic wave propagation with high stability and less numerical dispersion, and we can satisfy the boundary conditions theoretically. We conclude the CIP scheme is a very powerful technique to deal with geophysical problems such as accurate, high-frequency, full-wavefield simulation in models with highly inhomogeneous and complex topographic media.

References

[1] C. Cerjan, D. Kosloff, R. Kosloff and M. Reshef, A nonreflecting boundary condition for discrete acoustic and elastic wave equations, Geophysics, 50 (1985), 705-708.
[2] R. Clayton and B. Engquist, Absorbing boundary conditions for acoustic and elastic wave equations, Bull. Seism. Soc. Am., 67 (1977), 1529-1540.
[3] D. Kosloff, M. Reshef and D. Loewenthal, Elastic wave calculation by the Fourier method, Bull. Seism. Soc. Am., 74 (1984), 875-892.
[4] T. Kudoh, Magnetically driven jets from accretion disks. III. 2.5-dimensional nonsteady simulations for thick disk case, Astrophys. J., 508 (1998), 186-199.
[5] A. R. Levander, Fourth-order finite-difference P-SV seismograms, Geophysics, 53 (1988), 1425-1436.
[6] Y. Ogata, T. Yabe and K. Odagaki, An accurate numerical scheme for Maxwell equation with CIP-method of characteristics, Commun. Comput. Phys., 1 (2006), 311-335.
[7] H. Takewaki and T. Yabe, The cubic-interpolated pseudo particle (CIP) method: Application to nonlinear and multi-dimensional hyperbolic equations, J. Comput. Phys., 70 (1987), 353-372.
[8] J. Vireux, P-SV wave propagation in heterogeneous media: Velocity-stress finite-difference method, Geophysics, 51 (1986), 889-901.

[9] T.Yabe, T. Ishikawa, P. Y. Wang, T. Aoki, Y Kadota and F. Ikeda, A universal solver for hyperbolic equation by cubic-polynomial interpolation, II. Two- and three-dimensional solvers, Comput. Phys. Commun., 66 (1991), 233-242.
[10] T. Yabe and T. Aoki, A universal solver for hyperbolic equation by cubic-polynomial interpolation, I. One-dimensional solver, Comput. Phys. Commun., 66 (1991), 219-232.
[11] T. Yabe, F. Xiao and T. Utsumi, The constrained interpolation profile method for multiphase analysis, J. Comput. Phys., 169 (2001), 556-593.